ISBN-978-989-53228-8-6
39th MILAN International Conference on "Advances in Science, Engineering & Technology" (MASET-22)
Milan (Italy) Mar. 14-16, 2022

A New Model of Tandem Solar Cells

Mourad Talbi[1], Nawel Mensia[2] and Rached Ganouni[2]

[1]Laboratory of Nanomaterials and Systems for Renewables Energies (LaNSER), Center of Researches and Technologies of Energy of Borj Cedria, Hammam-Lif

[2]Laboratoire de Photovoltaic, Center of Researches and Technologies of Energy of Borj Cedria, Hammam-Lif

***Abstract*:** *The goal of this study consists in investigating the shading effect on a novel architecture of PVG (Photovoltaic Generator) introduced in this paper. This architecture is constituting of three PV modules in series connected. Two of them are constituting of amorphous silicon cells in series connected. The third module is constituting of monocrystalline silicon cells in series connected. This architecture is conceived as a PV concentrator where the two amorphous PV Modules are located in the lower position and the third one is located in the focus. The upper module absorbs the solar rays reflected by the two other modules to gain the maximum of solar energy. This architecture is introduced in order to solve problems existing with the tandem solar cell's architecture proposed in literature. Those problems are the mismatch between cells and both complicated fabrication and costs of tunnel junctions. In this paper, MATLAB/SIMULINK is used for modeling this architecture and studying its characteristics (I-V and P-V) in case of partial shading. It was found through this study that the maximum power provided by the PV concentrator, is influenced by the partial shading. To solve this partial shading problem, in this work, we make this new architecture as a solar tracker. The implementation of this solar tracker, is performed using arduino card.*

Keywords: *)concentrator, Focus, Photovoltaic Module, Shading, Solar Tracker, Arduino Card, Tandem Solar Cells*

1. Introduction

Silicon heterojunction solar cells (SHJ) dominate the photovoltaic market and this thanks to the high performance of power conversion. Indeed, they have the most stable and high PCE (Power Conversion Efficiency). Up to now, the highest PCE of the SHJ-interdigitated back contacts (IBC) solar cells reached 26.7%, nearly approaching the theoretical Shockley–Queisser (SQ) limitation of 29.4%. To break through this limit, Multi-Junction (MJ) devices constitute of two or three stacked subcells have been developed, which can fully use the sunlight by absorbing diverse parts of the solar spectrum [1].

Crystalline silicon solar cells dominate the photovoltaic market for many decades. The system components including cabling, inverters, and installation account for the foremost cost of photovoltaics, due to the fact that these costs are area dependent. Ameliorating the PCE is the most powerful means for reducing the levelized cost of electricity. The SHJ solar cells include $c - Si/a - Si$ [1–8], $c - Si/poly - Si$ [9–12], $c - Si/SiOx$ [13–18], and c-Si/MoOx [19, 20] Hetero-Junctions solar cells. SHJ solar cells represent the novel research direction thanks to their high performance.

The $a - Si{:}H/c - Si$ solar cells is constituting of a thin layer of highly doped amorphous hydrogenated silicon (a-Si:H), which is deposited on a moderately doped, mono-crystalline silicon wafer ($c - Si$). The low conductivity of doped a-Si:H needs the employment of a transparent, conductive layer (TCO) on top of the amorphous emitter, which minimizes resistive losses as well as reflective losses. Moreover, high efficiency features such as surface texturing, and the incorporation of a thin intrinsic $a-Si:H$ layer have been employed for improving the effectiveness [21]. Some of defects of mismatch between cells and tunnel junction costs and fabrication, exist in the tandem PV cells architecture [22]. For solving these defects, in this paper is established a novel Architecture of PV Generator (PVG) based on $a-Si:H/c-Si$ Materials. This PVG architecture is constituting of three PV modules in series connected. The modelling of this architecture is performed through $MATLAB/SIMULINK$ and this for taking in consideration some constraints when constructing this architecture. These constraints are the effect of the upper PV module on the two lower PV ones and also the cells number in the upper PV Module and the surface of each of them. In fact, we have to eliminate partial shading effect caused by the upper PV Module on the two lower PV ones and reducing the loss of sun lights reflected by those two lowers PV Modules. The findings shed new light on the effect of shading in the characteristics ($P-V$ and $I-V$) of the new architecture modeled using Matlab/Simulink. The rest of this paper is as follow: in part 2 we will detail the novel PVG architecture proposed in this work. In part 3, we will deal with the effect of the partial shading on $P-V$ and $I-V$ characteristics. In part 4, we will detail the Matlab-Simulation of the proposed PVG exposed to diverse Partial Shading Conditions In part 5, we will present and discuss the results obtained from Matlab/Simulink of this architecture for different values of insolation. Those results will be in terms of $I-V$ and $P-V$ characteristics. Finally, we will conclude in part 6.

2. The novel proposed PVG Architecture

The extreme efficiency of MJ (Multi − Junction) solar cells is based on having a total uniformity between the current of the different junctions and therefore working under optimal conditions (using a tunnel junction). In addition, it is necessary to match the network constant of all the layers to the substrate in order to have a significant crystalline quality [23]. Thus, in this paper we introduce a new tandem cell architecture. This architecture (Fig. 1) allows to solve the problems related to the tandem cells such as the coherence of current and network constant for each layer and the high manufacturing costs. As illustrated in Fig. 1, the new architecture is a parabolic concentrator made up of two receivers. Each receiver is formed by a number of solar cells based on amorphous and monocrystalline silicon.

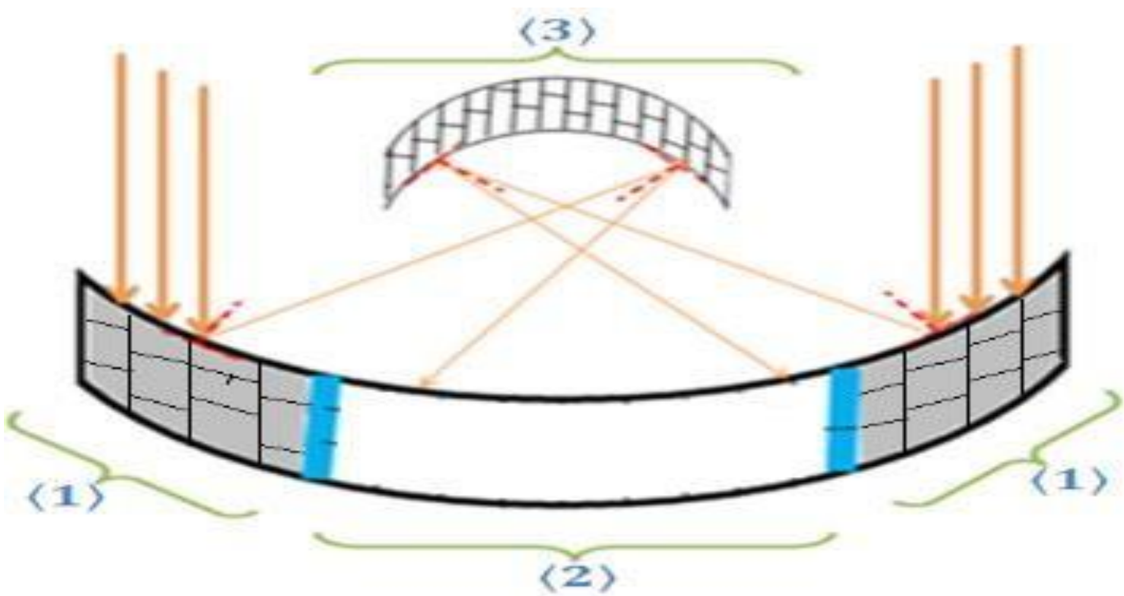

Fig. 1: New tandem solar cells model using parabolic concentrator.

The parabolic receiver in the lower position is formed by two regions numbered 〈**1**〉 and 〈**2**〉. The region 〈2〉 is formed by two separated parabolic rods connecting the two numbered regions 〈**1**〉 and does not contain any solar cells. The two regions numbere 〈**1**〉 are formed by series connected solar cells. Those cells are amorphous silicon ones. The receiver in upper position is formed only by a single region numbered 〈**3**〉 and containing a series connected solar cells which are monocrystalline silicon ones. The choice of the different locations of these amorphous and monocrystalline solar cells in this concentrator, is based on the fact that we want to maximize the absorption of the solar radiations (incidents and reflected). In fact, cells with short wavelengths (250 nm ~ 750 nm) are placed in the receiver located in the low position and cells with high wavelengths ($750\,nm \sim 1125\,nm$) are placed in the receiver located in the high position. Amorphous silicon $a-Si{:}H$ and crystalline silicon $c-Si$ solar cells own similar structure. They have an absorbent layer TiO_2, $p-n$ junction and reflective layer Al_2O_3 (Figure 2: (a) $a-Si{:}H$ single junction solar cells and (b) $c-Si$ single junction solar cells).

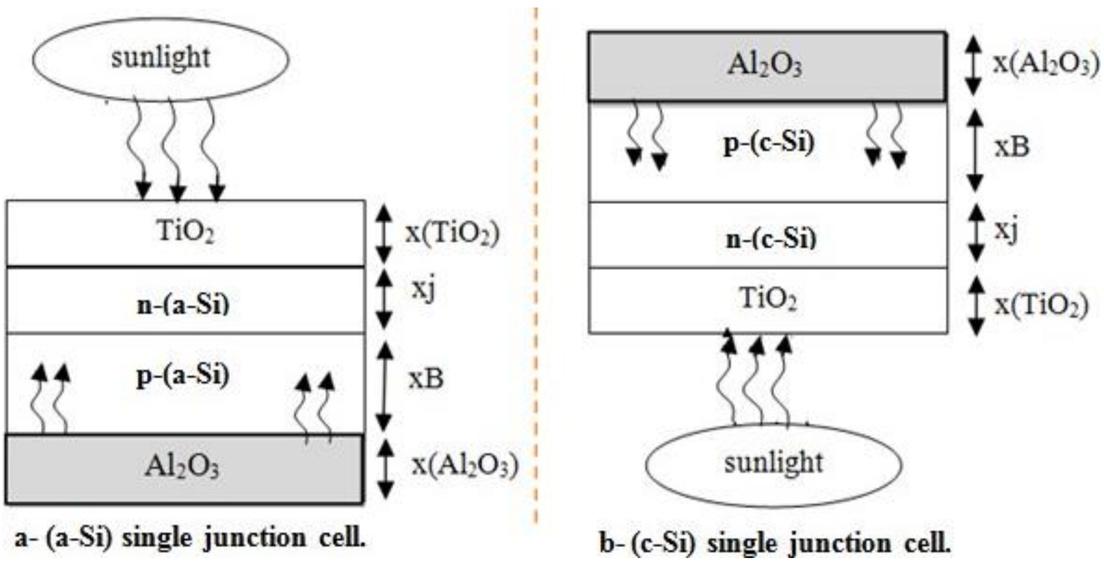

Fig.2: Structural model of single junction cell: (a) a-Si, (b) Si-c.

3. The partial shading effects

In this novel architecture, the PV Modules ⟨**1**⟩ in the lower positions can be shaded by the second parabolic receiver at the upper position. So, in section 4, we will deal with the effects of this shading on the characteristics $P-V$ and $I-V$ obtained from the lighting of the overall proposed parabolic trough concentrator.

4. Simulation of the proposed PV Generator under different partial shading conditions

In our simulations under MATLAB/SIMULINK and as previously mentioned, three PV Modules are employed in the proposed parabolic trough concentrator (Figures 1 and 3) where two PV modules are in lower position (numbered ⟨**1**⟩ in Fig. 1). The third PV Module is in the upper position, precisely in the Focus region (numbered ⟨3⟩ in Fig. 1). All of those PV Modules are in series connected. Each of the two PV modules numbered ⟨**1**⟩ contains six Amorphous PV cells in series connected. The third PV Module numbered ⟨3⟩ contains six Monocrystalline PV cells in series connected. In Figure 3 is illustrated the model under MATLAB/SIMULINK of the proposed parabolic trough concentrator. For modelling this model (Figure 3), we have used the PV Cell Model proposed in [24] and illustrated in Figure 5. The input of this PV Cell is the insolation and its outputs are both the voltage and the current (Figure 5). As previously mentioned, it can be a Amorphe or monocrystalline or polycrystalline PV cell. In Figure 4 is illustrated inside of one PV module used in the overall proposed Photovoltaic generator (Figure 3). In Figures 6 and 7 are presented both $I - V$ and $P - V$ characteristics and this for the three cases which are monocrystalline, polycrystalline and amorphous.

In Table 1 are listed the different parameters of one PV cell [24] employed in the model of the PV Generator proposed in this work. The type of the PV cell is Monocrystallin or Amorphous or Polycrystallin.

TABLE I: Parameters of the PV Cell used in both [24] and our GPV model

PV Cell parameter	Value
I_{sc}(A)	5.09
V_{oc}(V)	0.601
T(°C)	25

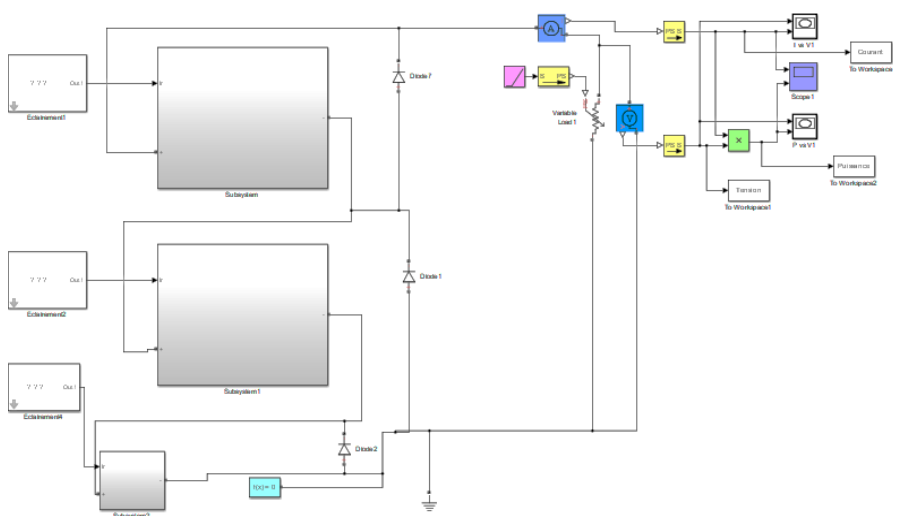

Fig. 3: The overall proposed photovoltaic generator under partial shading.

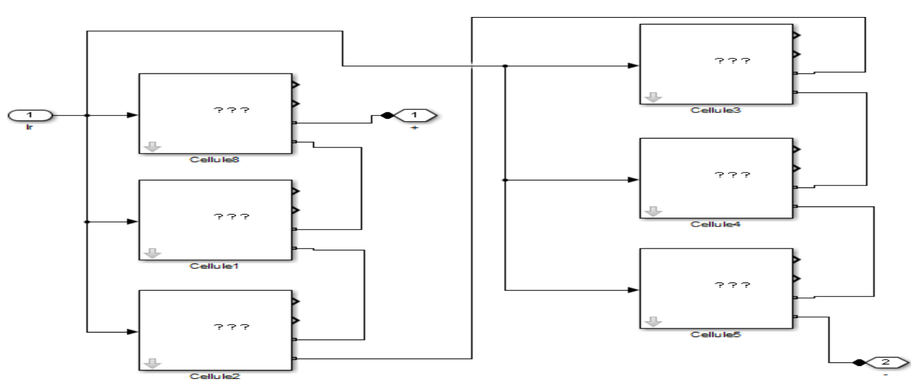

Fig. 4: Inside of one PV module used in the overall proposed Photovoltaic generator (Fig. 3).

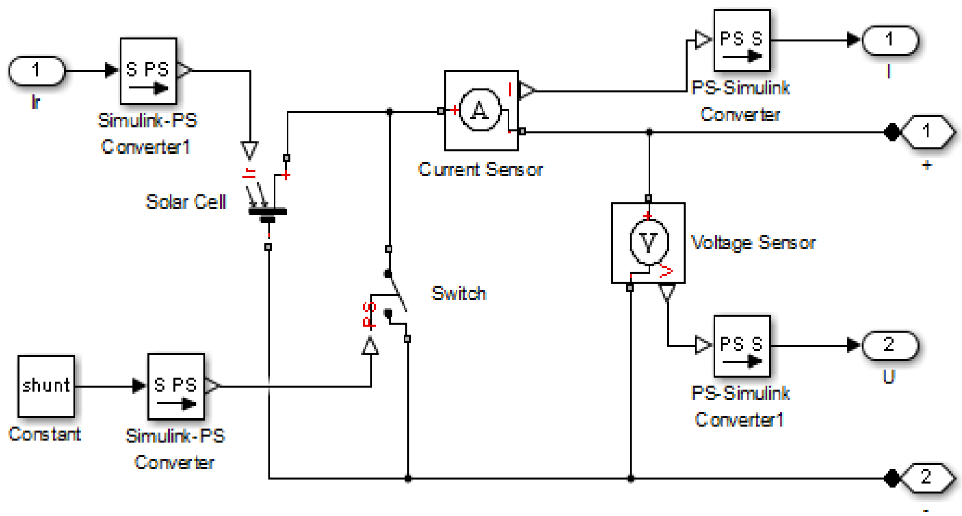

Fig. 5: Inside of the block of the PV Cell Model proposed in [24] and used in the overall proposed Photovoltaic Generator (Fig. 3).

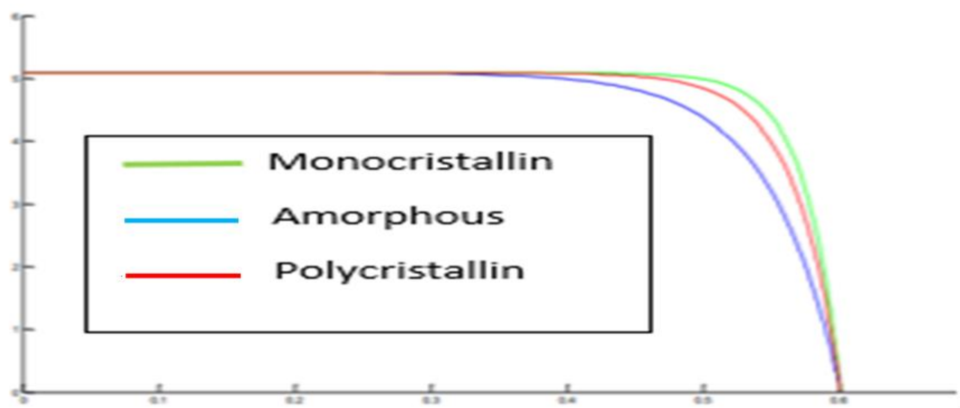

Fig. 6: I-V characteristics: curve in green color for monocristallin PV Cell, curve in blue color for Amorphous PV Cell, curve in red color for Polycrystallin PV Cell.

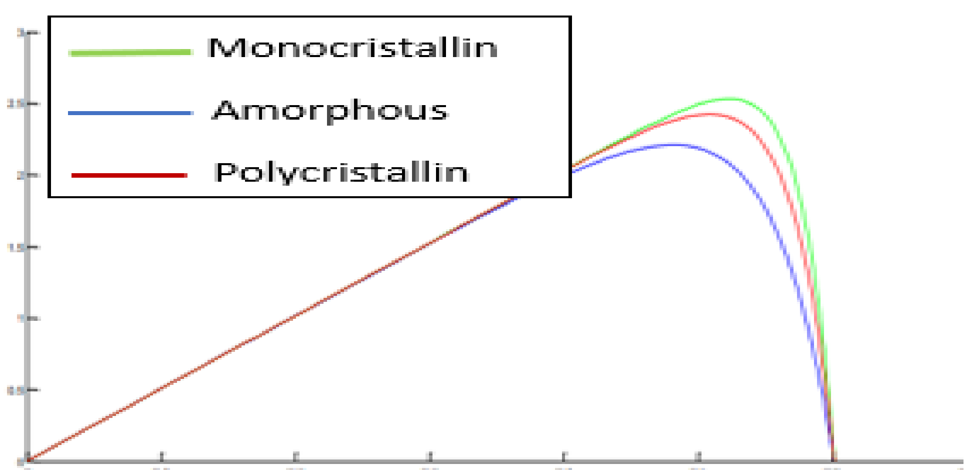

Fig. 7: P-V characteristics: curve in green color for monocristallin PV Cell, curve in blue color for Amorphous PV Cell, curve in red color for Polycristallin PV Cell.

5. Results and discussion

In this section are presented the results obtained from simulations under MATLAB/SIMULINK of the proposed Model of the parabolic trough concentrator. Those results are different P-V and I-V characteristics (Figs. 8, 9) for diverse values of insolation (with and without shading).

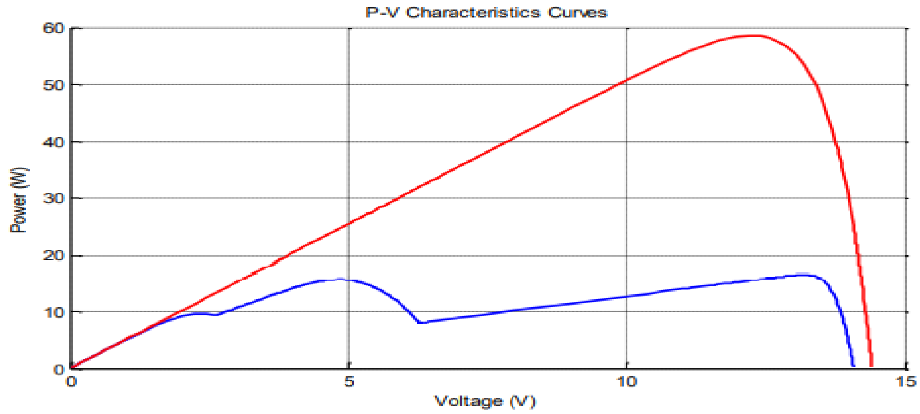

(a)

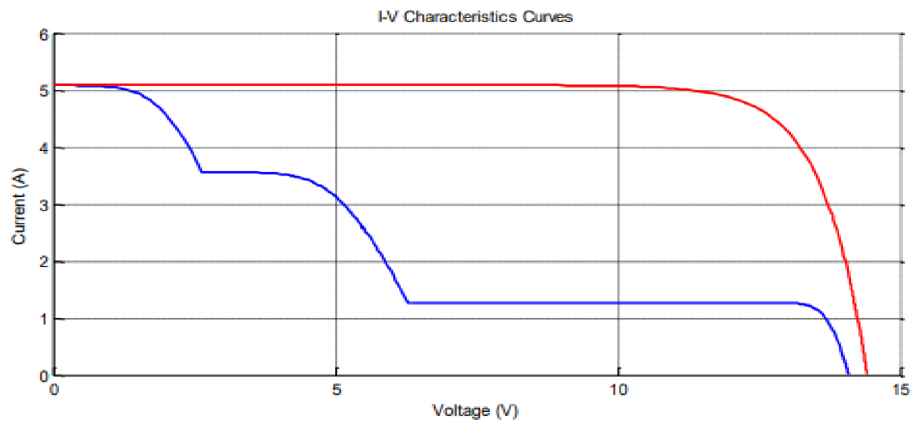

(b)

Fig. 8: Characteristics P-V (*a*) and I-V (*b*) (Without Shading in Red color ([1000, 1000, 1000] W/m^2) and with Shading in Blue Color ([1000, 700, 250] W/m^2).

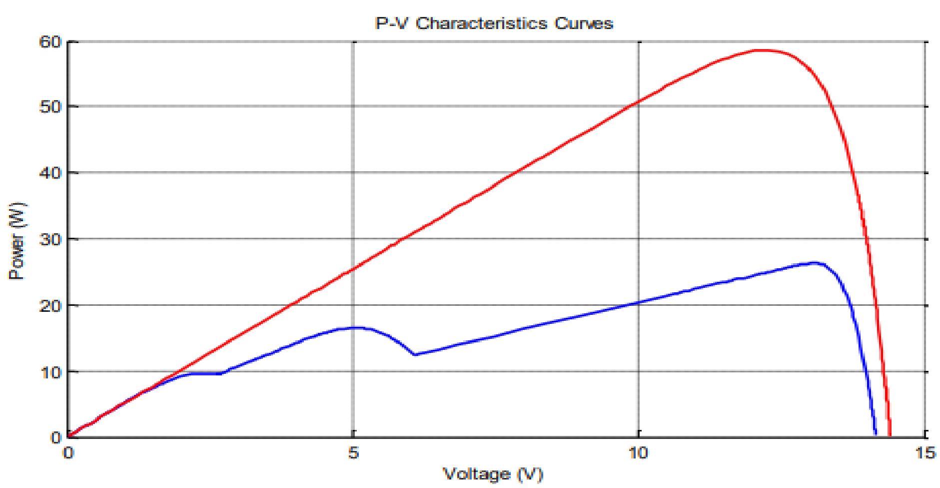

(a)

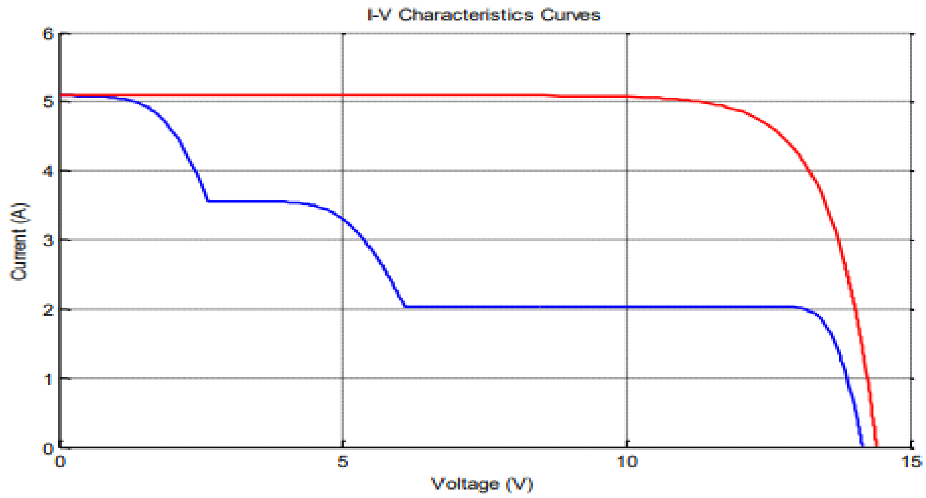

(b)

Fig. 9: Characteristics P-V (*a*) and I-V (*b*) (Without Shading in Red color ([1000, 1000, 1000] W/m^2) and With Shading in Blue Color ([1000, 700, 400] W/m^2).

These different characteristics show that the maximum PV power is affected by the partial shading. Three local peaks appear on the P-V and I-V characteristics (Figs 8-9). Those peaks vary with the level of the partial shading. During partial shading, each module is exposed to different irradiances. Consequently, each Module has its own maximum (peak) power. The solution to completely overcome the problem of shading is to make this novel architecture of PV Generator, as a solar tracker. In the following sub-section we will detail the implementation of a solar tracker using arduino card.

5.1. A Solar Tracker Implimentation

5.1.1. The employed materials and hardware

In this work, we want to employ the stepper motor used in [25] instead of (28BYJ-48 Stepper Motor) used for the implementation of the solar tracker proposed and detailed in [26]. So, for implementing this solar tracker, we have used the electronic components:

- Stepper Motor used in [25],
- Photo Resistor: Product Link: Photo Resistor,
- Resistor: 220ohm – Product Link: E-Projects – 220 Ohm Resistors – 1/4 Watt – 5% – 220R (100 Pieces).

5.1.2. The Stepper Motor Control

The A4988 is a microstepping driver used for controlling a bipolar Stepper Motor which has built-in translator for easy operation. Therefore, one can control the Stepper Motor with just 2 pins from controller [25], one for controlling the steps and the other for controlling the rotation direction.

Fig.10: The A4988 Stepper Driver.

This Driver provides five diverse step resolutions which are as follow: sixteenth-step, full-step, quarter-step, haft-step and eight-step. It also owns a potentiometer in order to adjust the current output, over-temperature thermal shutdown and crossover-current protection. Its logic voltage varies from 3 to 5.5*V* and the maximum current per phase is 1*A* without heat sink or cooling and 2*A* if good addition cooling is provided [25].

In Fig. 11, is illustrated the complete circuit schematics of the operating the stepper motor used in [25] and also in this work.

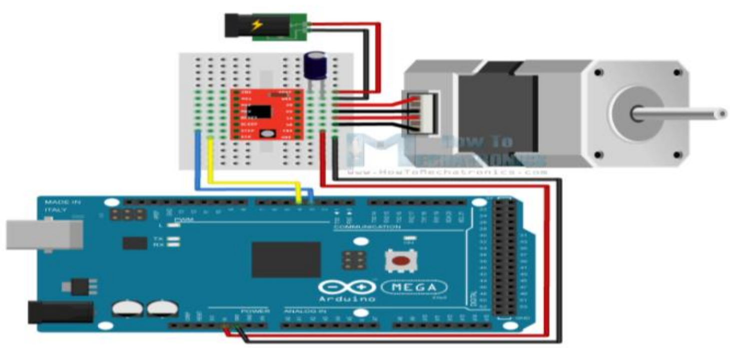

Fig.11: The overall system of stepper motor operation [2].

5.1.3. Programming the stepper motor and the solar tracker

In this work, for programming the stepper motor and the solar tracker we have used the Arduino code given in [26].

6. Conclusion

In this paper, is proposed a novel architecture of a PVG, constitutes of three PV modules in series connected. Two of them are constituting of amorphous silicon cells in series connected and the third one by monocrystalline silicon cells. This new architecture is conceived as a PV concentrator where the two Amorphous PV Modules are located in the lower position and the third one is located in the upper position precisely in the Focus. This architecture is proposed for solving problems presenting in the architecture of tandem solar cells proposed in literature. Those problems are the mismatch between cells and the tunnel junction costs and fabrication. The role of the upper Module consists in absorbing the solar rays reflected by the two other ones and this for gaining the maximum of solar energy. In this work, we use MATLAB/SIMULINK for modelling this architecture of a PV Generator and studying their characteristics (I-V and P-V) in case of partial shading. In fact, the two lower PV modules are partially shaded by the upper PV one. The solution to completely solve this problem, consists in making this PVG architecture dynamic as a solar tracker.

References

[1] X. Li, Q. Xu, L. Yan, et al., "Silicon heterojunction-based tandem solar cells: past, status, and future prospects," Nanophotonics, vol. 10, no. 8, 2021, https://doi.org/10.1515/nanoph-2021-0034.

[2] K. Masuko, M. Shigematsu, T. Hashiguchi, et al., "Achievement of more than 25% conversion efficiency with crystalline silicon heterojunction solar cell," IEEE J. Photovoltaics, vol. 4, no. 6, pp. 1433–1435, 2014.
https://doi.org/10.1109/JPHOTOV.2014.2352151

[3] Nakamura, N. Asano, T. Hieda, C. Okamoto, H. Katayama, and K.Nakamura, "Development of heterojunction back contact Si solar cells," IEEE J. Photovoltaics, vol. 4, no. 6, pp. 1491–1495, 2014.
https://doi.org/10.1109/JPHOTOV.2014.2358377

[4] M. Taguchi, A. Yano, S. Tohoda, et al., "24.7% record efficiency HIT solar cell on thin silicon wafer," IEEE J. Photovoltaics, vol. 4, no. 1, pp. 96–99, 2014.
https://doi.org/10.1109/JPHOTOV.2013.2282737

[5] D. Adachi, J. L. Hernández, and K. Yamamoto, "Impact of carrier recombination on fill factor for large area heterojunction crystalline silicon solar cell with 25.1% efficiency," Appl. Phys. Lett., vol. 107, no. 23, p. 233506, 2015.
https://doi.org/10.1063/1.4937224

[6] K. Yoshikawa, H. Kawasaki, W. Yoshida, et al., "Silicon heterojunction solar cell with interdigitated back contacts for a photoconversion efficiency over 26%," Nat. Energy, vol. 2, no. 5, 2017.
https://doi.org/10.1038/nenergy.2017.32

[7] K. Yoshikawa, W. Yoshida, T. Irie, et al., "Exceeding conversion efficiency of 26% by heterojunction interdigitated back contact solar cell with thin film Si technology," Sol. Energy Mater. Sol. Cells, vol. 173, pp. 37–42, 2017.
https://doi.org/10.1016/j.solmat.2017.06.024

[8] J. B. Heng, J. Fu, B. Kong, et al., "23% high-efficiency tunnel oxide junction bifacial solar cell with electroplated Cu gridlines," IEEE J. Photovoltaics, vol. 5, no. 1, pp. 82–86, 2015.
https://doi.org/10.1109/JPHOTOV.2014.2360565

[9] F. Feldmann, M. Simon, M. Bivour, C. Reichel, M. Hermle, and S. W. Glunz, "Efficient carrier-selective p- and n-contacts for Si solar cells," Sol. Energy Mater. Sol. Cells, vol. 131, pp. 100–104, 2014.
https://doi.org/10.1016/j.solmat.2014.05.039

[10] A. Richter, J. Benick, F. Feldmann, A. Fell, M. Hermle, and S. W. Glunz, "n-Type Si solar cells with passivating electron contact: identifying sources for efficiency limitations by wafer thickness and resistivity variation," Sol. Energy Mater. Sol. Cells, vol. 173, pp. 96–105, 2017.
https://doi.org/10.1016/j.solmat.2017.05.042

[11] F. Haase, C. Hollemann, S. Schäfer, et al., "Laser contact openings for local poly-Si-metal contacts enabling 26.1%-efficient POLO-IBC solar cells," Sol. Energy Mater. Sol. Cells, vol. 186, pp. 184–193, 2018.

https://doi.org/10.1016/j.solmat.2018.06.020

[12] F. Haase, S. Schafer, C. Klamt, et al., “Perimeter recombination in 25%-efficient IBC solar cells with passivating POLO contacts for both polarities,” IEEE J. Photovoltaics, vol. 8, no. 1, pp. 23–29, 2018.

https://doi.org/10.1109/JPHOTOV.2017.2762592

[13] K. Ding, U. Aeberhard, F. Finger, and U. Rau, “Silicon heterojunction solar cell with amorphous silicon oxide buffer and microcrystalline silicon oxide contact layers,” Phys. Status Solidi Rapid Res. Lett., vol. 6, no. 5, pp. 193–195, 2012.

https://doi.org/10.1002/pssr.201206030

[14] K. Ding, U. Aeberhard, F. Finger, and U. Rau, “Optimized amorphous silicon oxide buffer layers for silicon heterojunction solar cells with microcrystalline silicon oxide contact layers,” J. Appl. Phys., vol. 113, no. 13, p. 134501, 2013.

https://doi.org/10.1063/1.4798603

[15] K. Ding, U. Aeberhard, V. Smirnov, B. Holländer, F. Finger, and U. Rau, “Wide gap microcrystalline silicon oxide emitter for a-SiOx:H/c-Si heterojunction solar cells,” Jpn. J. Appl. Phys., vol. 52, no. 12R, p. 122304, 2013.

https://doi.org/10.7567/JJAP.52.122304

[16] A. Richter, F. Lentz, M. Meier, F. Finger, and K. Ding, “Light management in planar silicon heterojunction solar cells via nanocrystalline silicon oxide films and nano-imprint textures,” Phys. Status Solidi, vol. 213, no. 7, pp. 1976–1982, 2016.

https://doi.org/10.1002/pssa.201533024

[17] M. Pomaska, A. Richter, F. Lentz, et al., “Wide gap microcrystalline silicon carbide emitter for amorphous silicon oxide passivated heterojunction solar cells,” Jpn. J. Appl. Phys., vol. 56, no. 2, p. 022302, 2017.

https://doi.org/10.7567/JJAP.56.022302

[18] T. Krajangsang, S. Inthisang, J. Sritharathikhun, et al., “An intrinsic amorphous silicon oxide and amorphous silicon stack passivation layer for crystalline silicon heterojunction solar cells,” Thin Solid Films, vol. 628, pp. 107–111, 2017.

https://doi.org/10.1016/j.tsf.2017.03.010

[19] C. Battaglia, S. M. de Nicolás, S. De Wolf, et al., “Silicon heterojunction solar cell with passivated hole selective MoOx contact,” Appl. Phys. Lett., vol. 104, no. 11, p. 113902, 2014.

https://doi.org/10.1063/1.4868880

[20] J. Geissbühler, J. Werner, S. Martin de Nicolas, et al., “22.5% efficient silicon heterojunction solar cell with molybdenum oxide hole collector,” Appl. Phys. Lett., vol. 107, no. 8, p. 081601, 2015.

https://doi.org/10.1063/1.4928747

[21] Meng F., Shi J., Shen L., Zhang L., Liu J., Liu Y., Yu J., Bao J., Liu Z.. (2017). Characterization of transparent conductive oxide films and their effect on amorphous/crystalline silicon heterojunction solar cells. Japanese Journal of Applied Physics 56: 04CS09. https://doi.org/10.7567/JJAP. 56.04C S09

[22] Si F., Isabella O., Zeman M.. (2017). Too many junctions? A case study of multijunction thin-film silicon solar cells. Advanced Sustainable Systems 1(10). https://doi.org/10.1002/adsu.201700077

[23] Masafumi Y. (2003). III–V compound multi-junction solar cells: Present and future. Solar Energy Materials & Solar Cells 75(1-2): 261-269. https://doi.org/10.1016/S0927-0248(02)00168-X

[24] www.ac-clermont.fr/disciplines/index.php?id=5219

[25] https://howtomechatronics.com/tutorials/arduino/how-to-control-stepper-motor-with-a4988-driver-and-arduino/

[26] Arduino based Solar Tracker – Stepper Motor & Light Resistor Tutorial – EEEnthusiast